Cross-sensor change detection over a forested landscape: Options to enable continuity of medium spatial resolution measures

Michael A. Wulder*, Christopher R. Butson, and Joanne C. White

Canadian Forest Service (Pacific Forestry Centre), Natural Resources Canada, Victoria, British Columbia, Canada

* Corresponding author:
506 West Burnside Rd., Victoria, BC V8Z 1M5;
Phone: 250-363-6090; Fax: 250-363-0775; Email: mike.wulder@nrcan.gc.ca

Pre-print of published version.
Reference:
Wulder, M.A., Butson, C.R., White, J.C. 2008. Cross-sensor change detection over a forested landscape: Options to enable continuity of medium spatial resolution measures. Remote Sensing of Environment, 112: 796–809.

DOI.
DOI: http://doi:10.1016/j.rse.2007.06.013

Disclaimer:
The PDF document is a copy of the final version of this manuscript that was subsequently accepted by the journal for publication. The paper has been through peer review, but it has not been subject to any additional copy-editing or journal specific formatting (so will look different from the final version of record, which may be accessed following the DOI above depending on your access situation).

Abstract

Landsat data have been widely used for change detection studies of forest ecosystems. Technical issues related to the longevity and quality of the Landsat-5 and -7 instruments prompted this investigation into how data from other sensors may be integrated with the existing Landsat image archive. Change maps indicating the location and extent of stand replacing disturbances occurring between 1999 and 2004 were developed using a rank-order change detection approach. The near infrared (NIR) band from an image representing initial stand conditions (T1: Landsat 7 ETM+), and the NIR band of images acquired on subsequent dates and with different sensors (T2: ASTER, SPOT-4, and Landsat-5 TM) were selected, essentially acting as three different T2 images. Pair-wise comparisons between the T1 image and each of the T2 images required the pixel values to be sorted, ranked, and differenced; a threshold was then applied to the difference values to identify the stand replacing disturbances. The rank-order change detection approach precluded the need for an additional image normalization process. When compared to a manually interpreted map of change events, the output from the ASTER, SPOT-4, and Landsat-5 TM data were all equally effective in identifying all of the stand replacing disturbances that occurred between 1999 and the year of T2 image acquisition, and errors of commission were minimal. Important logistical limitations to cross-sensor change do exist however and include the lack of spatially or temporally extensive image archives for sensors other than Landsat, incompatible image footprints, and data cost and policy. This rank-order change detection approach is suitable for applications involving multi-temporal datasets where problems may exist due to image normalization, cross-sensor radiometric calibration, or unavailability of a desired sensor type.

Key words: Landsat, SPOT, ASTER, land cover, forest, change detection, cross-sensor, continuity, monitoring, rank-order, LDCM, OLI, polygon decomposition

1.0 Introduction

Globally, forest ecosystems are under pressure from urban and agricultural expansion, fuel extraction, harvesting activities, and climate change (Hansen et al., 2001). Together, these factors result in high rates of forest change and subsequent monitoring challenges (e.g. Desclée et al., 2006; Hayes and Cohen, 2007). For instance, between 1990 and 2000, global forest area declined at a rate of 8.9 million hectares per year, and between 2000 and 2005, global forest area decreased by approximately 7.3 million hectares per year (Food and Agriculture Organization of the United Nations, 2005). Changes in forest cover have significant ecological, economic, and social implications, particularly in nations such as Canada where 41% of the total landmass (402.1 million hectares) is forested (Natural Resources Canada, 2006). The pressures upon forests have resulted in a broad range of national, regional, and international initiatives promoting sustainable forest management. These initiatives have in turn generated new information needs and increased reporting requirements. The requirement to collect information on forest change over large areas with an increasing level of detail has resulted in the use of remotely sensed data for forest monitoring programs (Wulder et al., 2004; Hickey et al., 2005).

Remotely sensed data can play a major role in forest monitoring programs; the timing and spatial extent of changes to forest cover may be captured at a range of spatial scales with remotely sensed data (Malingreau, 1993; Foody, 2003, Treitz and Rogan, 2004). The majority of forest monitoring research has relied on data from medium spatial resolution sensors such as Landsat-5 Thematic Mapper (TM) and Landsat-7 Enhanced Thematic Mapper Plus (ETM+) (Franklin and Wulder, 2002). The insightful and well integrated assemblage of Landsat's spectral, spatial, and temporal resolutions, combined with its extensive archive and relative low cost have resulted in an invaluable data source for change detection research (Woodcock et al., 2001; Cohen and Goward, 2004). The Landsat program has provided earth observation data to meet a wide range of information needs since 1972 (Mack, 1990). Unfortunately, temporal and spatial discontinuities in the extensive 34-year archive of Landsat data are increasingly probable. The failure of the Scan Line Corrector onboard Landsat-7 in 2003, (Markham et al., 2004) and problems with the solar array drive mechanism onboard Landsat-5 in 2005 (Frederick, 2005), coupled with the lack of formalized plans for a successor in the Landsat series of earth observation satellites (Goward and Skole, 2005), places an element of risk in reliance upon Landsat sensors for long-term forest monitoring programs.

In this paper we present a multi-sensor change detection approach that facilitates the use of remotely sensed data collected from several medium spatial resolution sensors, including ASTER, SPOT-4, and Landsat-5. The ASTER and SPOT-4 data sources have different spatial and spectral resolutions than TM and ETM+ data, and the method presented demonstrates how these data sources can be used in conjunction with an existing Landsat image archive, to capture stand replacing changes in forest ecosystems over time.

1.1 Change detection in forest ecosystems

Forest changes are generally caused by three forces: growth and evolutionary development; natural forces such as flooding, fire, insects and disease; and anthropogenic changes such as harvesting, thinning, or burning (Gong and Xu, 2003). These changes are manifested over a variety of spatial and temporal scales and the methods to detect these changes should be carefully considered, especially when using remotely sensed data sources. Change detection in forest environments has been undertaken using a wide variety of remotely sensed data sources. As previously indicated, forest change detection studies have relied on Landsat imagery to detect forest change, including insect-related disturbances (Price and Jakubauskas, 1997; Allen and Kupfer, 2001; Falkenstrom and Ekstrand, 2002; Skakun et al., 2003; Wulder et al., 2006), and stand replacing disturbances such as harvesting (Wilson and Sader, 2002; Jin and Sader, 2005; Healey et al. 2006a; Healey et al., 2006b), and fire (Rogan et al., 2002; McMichael et al., 2004; Epting et al., 2005).

Other medium resolution sensors have also been used for change detection studies in forest environments. For example, SPOT multispectral data have been used to detect forest defoliation (Muchoney and Haack, 1994), damage caused by inundation of forest ecosystems (Michener and Houhoulis, 1997), harvesting (Desclée et al., 2006), as well as for more general land cover change applications (Nemmour and Chibani, 2006; Prenzel and Treitz, 2006). Studies using ASTER data for change detection are less common, largely as a result of ASTER's smaller footprint and limited archive; however, recently the use of ASTER for forestry-related applications has begun to emerge in the literature (Muukkonen and Heiskanen, 2005; Fedpausch et al., 2006; Heiskanen, 2006).

The state-of-the-art in remote sensing change detection methods have been extensively reviewed and the relative strengths and weakness of these approaches are well documented (Mas, 1999; Gong and Xu, 2003; Coppin et al., 2004; Lu et al., 2004; Coops et al., 2006). Singh (1989) broadly grouped change detection approaches into either mathematical analyses of spectral differences between two images, or the more commonly applied post-classification comparisons. The former group of approaches includes image algebra, regression or correlation, and vegetation indices and principal component analysis (Gong and Xu, 2003).

The main objective of this study is to capture stand-replacing disturbances across a forested landscape using data from multiple remote sensing platforms. A forest stand represents the smallest unit on which a forest resource is mapped when minimum mapping unit and resource management decisions are made (Gong and Xu, 2003). A stand replacing disturbance is considered one in which all the forest cover within a given stand is either removed or destroyed at a single point in time (Cohen et al., 2002). Generally, these events are large enough to be visible on an image with a moderate spatial resolution. Examples of stand replacing disturbances include wildfire and clearcut logging. In this study, we apply a rank-order change detection procedure and derive change maps from ASTER, SPOT-4, and Landsat-5 TM data using baseline Landsat-7 ETM+ imagery (using NIR bands). Comparing the outputs of the process to a manually interpreted validation dataset assesses the effectiveness of the rank-order change detection process. Finally, we demonstrate how the change results generated from this method could be used to update an existing land cover product.

2.0 STUDY SITE

The study site is centered at 54° 45’ 00” N latitude 123° 30’ 00” W longitude and is located approximately 60 km northeast of Fort St. James, British Columbia, Canada (Figure 1). The site is located in the Prince George Forest District, which is positioned in the center of the province in the Sub-Boreal Spruce (SBS) biogeoclimatic zone (Medinger and Pojar, 1991). This zone spreads across the rolling terrain of the British Columbia interior plateau. The climate in this region is characteristically extreme, being hot and moist in the short summer months and cold with a large accumulation of snow in the winter months. Frequent thunderstorms are common in this zone, creating a fire hazard in the summer months. Forests here are dominated by white spruce (Picea glauca), subalpine fir (Abies lasiocarpa), and occasionally black spruce (Picea mariana), lodgepole pine (Pinus contorta var. latifolia), and Douglas-fir (Pseudotsuga menziesii) in drier parts of the zone. Trembling aspen (Populus tremuloides) and paper birch (Betula papyrifera) are present on moist and dry upland sites (Medinger and Pojar, 1991). This site was chosen because there was active logging in this area between 1999 and 2005.

3.0 DATA AND METHODS

3.1 Image Data

The Landsat-7 ETM+, ASTER, SPOT-4, and Landsat-5 TM images used in this study are all located within Path 49, Row 22 of the Landsat World Reference System (WRS) (Figure 1). These images were chosen based on coincident coverage for each sensor during the summer growing season, appropriate temporal coverage to perform change detection analysis, and coverage with minimal cloud/haze contribution. Given these criteria, it was not possible to acquire data with the same temporal coverage (due to a lack of systematic collection and archiving of non-Landsat data). The T1 image represented initial forest conditions and was acquired from the Landsat 7 ETM+ sensor on September 12, 1999 as a Level 1G product (at-sensor radiance, geometrically corrected) (Irish, 2000). The T2 images represented change conditions and were collected, as available from ASTER, SPOT-4, and Landsat-5 sensors in 2000, 2003, and 2004 respectively (Table 1). The SPOT-4 image was acquired as an orthorectified Level 1A product (scaled at-sensor radiance) (SPOT Image, 2006). The ASTER data was acquired as a Level 1B product (scaled at-sensor radiance and geometrically corrected). The Landsat-5 TM data were acquired from the USGS in Level 1 format processed using the National Land Archive Production System (United States Geological Service, 2007). The required image processing and subsequent analysis steps are outlined in Figure 2.

3.2 Image pre-processing

The Landsat-7 ETM+ image is used as the reference scene for initial (T1) forest conditions (pre-harvest). This image was georeferenced to Universal Transverse Mercator (UTM) Zone 10, using a nearest-neighbor, first-order polynomial transformation from the geographic coordinates provided in the header files, in conjunction with vector coverages from the Canadian National Topographic Database (NTDB) (Geomatics Canada, 1996). Using the Landsat-7 ETM+ image as the master, an image-to-image registration was then performed between each of the other images and the T1 image. Each of the other three images representing the changed forest conditions (T2: ASTER, SPOT-4, and Landsat-5 TM) was corrected to the reference image using a minimum of 16 ground control points and a first-order polynomial. The root-mean-square (RMS) error was less than 15 m for each image-to-image correction. As part of the image registration process, the T2 images were resampled from their original spatial resolution (Table 1), using a nearest neighbor algorithm, to a 30m spatial resolution to match the spatial resolution of the Landsat-7 ETM+ T1 image. The final step in the pre-processing stage was to extract a common, cloud-free area over all four images, suitable for analysis. The resultant area selected was 420 by 650 pixels (approximately12.6 km by 19.5 km) (Figure 1).

3.3 Image normalization and change detection

An ordinal conversion method of assigning ranks to pixel values was used to normalize the temporal sequence of imagery as per Nelson et al. (2005) (Figure 3). This approach to image normalization does not require extensive information on scene properties, nor does it require subjective determination of reference values, both of which are commonly associated with other image normalization procedures. Using an ordinal ranking approach, each pixel is assigned a new value based on its reflectance value, relative to all other reflectance values in the image. The concept of change detection implies that multiple images are compared to identify changes on the landscape that have occurred over time. The advantage of the ordinal ranking approach to image normalization is that the global characteristics of the distributions of pixel values in each image are matched (e.g., distributions will have the same range in values), thereby improving the detection of change events (Nelson et al., 2005).

Only the near-infrared (NIR) band from each sensor was used in the analysis, as this band was common to all four sensors used in this study, and has documented sensitivity to vegetation chlorophyll content (Jensen, 2000). Following the approach presented in Figure 3, the pixel values in the NIR channel for the T1 and T2 images were extracted to a flat text file and sorted in ascending order. Ranks were then assigned to each pixel value and when the same pixel value was counted more than once, tied ranks were assigned (Burt and Barber, 1996) as shown in Figure 3. As per Nelson et al. (2005), it was understood that exposed areas (e.g., new harvest blocks) are high in the NIR (brightest) and would have the high ordinal rank values; conversely forested areas appear darker (as captured in the NIR) and have the lower rank values. The trends captured in each image with the ordinal rank values are then compared between images (by differencing the two image); areas where there has been no change will have ranks that match, or are similar, in the ordinal space, and commensurate rank-order difference values that are zero or close to zero. Conversely, areas with change will have different rank-order values for each image, and consequently will have differences in rank-order values that are greater or less than zero, with the magnitude of the difference varying with type of change that has occurred. In this manner, change is identified as the relative difference between two ordinal ranked images. This approach capitalizes upon the global characteristics of the distributions of pixel values for the image pairs. The change detection and image normalization are integrated through the rank-order differencing, enabling cross-sensor change detection. Based on image dimensions and the number of pixels in each image used in this analysis (which were constant - as all images had the same spatial extent and the same pixel spatial resolution), possible rank values ranged from 1 to 273000.

Once a rank image was generated for the T1 image and the T2 images, the T1 image was subtracted from each of the T2 rank images (i.e., the rank values of the T1 image were subtracted from the T2 image at each pixel location). In order to reduce noise and to focus upon stand-replacing disturbances, a 3 by 3 modal filter was applied to each thresholded change map resulting in an approximate 1 ha minimum mapping unit (MMU).

3.4 Calibration and Validation

The British Columbia Ministry of Forests and Range provided the forest inventory data for the study area, which was compiled following the specifications for production of a vegetation resources inventory (VRI) from aerial photographs collected on various dates ranging from 1954 to 2005 (Resources Inventory Committee, 2002). The Ministry of Forests and Range also provided an update layer containing information on forest harvesting activities between 1999 and 2005. This update layer is generated by the Ministry using a change detection process and two dates of Landsat imagery, and is used by the Ministry as a quality assurance tool for auditing the currency of the inventory data (British Columbia Ministry of Forests and Range, 2007).

To facilitate the production of a set of calibration and validation data for this study identifying all of the stand replacing disturbances in the area of interest between 1999 and 2005, the NIR bands from the Landsat-7 ETM+, ASTER, SPOT-4, and Landsat-5 TM data were loaded into the viewing platform for the manual delineation of change. Using both the inventory data and the update layer supplied by the Ministry of Forests as guides, stand replacing disturbance events were manually interpreted from each of the T2 images and labeled with the year of the T2 image in which they were detected. For example, stand replacing disturbances identified in the 2003 SPOT-4 image were labeled as "2003"; however, these disturbances could have occurred between 2000 (after the collection of the ASTER image) and 2003. A summary of the manually interpreted stand replacing disturbance events is provided in Table 2. There were 31 stand replacing disturbances in the study area between 2000 and 2004 (Figure 4). A polygon decomposition process (Wulder and Franklin, 2001) was used to identify the number and area of forest inventory polygons impacted by stand replacing disturbance events (Table 2). Polygon decomposition is a process enabling the consideration of pixel values falling within a given polygon. Polygon decomposition, in this case, uses the vector VRI polygons and the manually delineated stand replacing disturbance polygons to organize and consider the change detection results.

To determine the threshold range that corresponded to the stand replacing disturbance events, the manually delineated disturbances were used as a mask, and all of the pixel values from each of the differenced image pairs under the mask were extracted. For the purposes of calibration, 10% of these extracted pixel values were then selected at random and used in an iterative process to determine the rank-order threshold value. After the threshold was determined, the pixels with values corresponding to the threshold range were extracted from the rank-order difference image, placed in a separate data layer, and labeled as stand replacing disturbance events. These disturbance events were then compared against the manually delineated disturbance polygons. Since each of the T2 images was acquired in a different year, the objective of the validation was to determine the effectiveness with which the stand replacing disturbances that occurred between T1 and T2 were detected. The change events identified through the rank-order change process were then decomposed to the forest inventory polygons to determine if all of the stands replacing events occurring in any given year were correctly identified. Validation is therefore conducted at the polygon level as opposed to the pixel level (Healey et al., 2006b).

3.5 Land cover update

The production of land cover maps with medium spatial resolution imagery is common and is considered reliable and operational (Franklin and Wulder, 2002). At present, the focus of many applications is the update of these land cover products to reflect changes in land cover over time (Langevin and Snow, 2004; Feranec et al., 2007). The outputs of the rank-order change detection process used in this study can be applied to update an existing land cover product. To demonstrate this, a portion of an existing land cover product, corresponding to the study area, was updated. The original land cover product was created for the Earth Observation for Sustainable Development of Forests (EOSD) project using Landsat-7 ETM+ to represent land cover circa 2000 (Wulder et al., 2003). GIS processing can be used to update the EOSD product with the stand replacing disturbances identified from the rank-order change detection process.

4.0 RESULTS

4.1 Rank-order change detection

Each of the T2 images was processed separately according to the methods outlined in Figures 2 and 3. The rank-order process normalized the distributions of the NIR band for the images (Figure 5) and thereby eliminated the need to use a more complex radiometric normalization process. The ranks of the T1 image were subtracted from the ranks of each of the T2 images. The distributions of the rank difference values for each of the T1 and T2 image pairs are shown in Figure 5. Three scenarios were expected and observed: negative values would be found where the T1 image had a higher rank than the T2 image (indicating forest growth); positive values would be found where the T2 image had a higher rank than the T1 image (indicating forest depletion); and values close to zero would be found where there was no or minimal change.

4.2 Threshold development

Using the manually interpreted stand replacing disturbances as a mask, the pixel values representing the rank-order difference between the Landsat-7 ETM+ image (1999) and the ASTER (2000), SPOT-4 (2003), and Landsat-5 TM (2004) images were extracted. Figure 6 shows the distribution of ordinal-rank difference values corresponding to these manually interpreted stand replacing disturbances for each image pair. These distributions indicate that conditions within a stand replacing disturbance are not homogenous and this is in keeping with our understanding of operational forestry. Harvested areas are often an assemblage of leave patches (groups of standing trees left behind for various management or logistical reasons), other intact vegetation, slash piles, landings, and roads – resulting in high spectral variability. A threshold range is applied to the rank difference image to identify the majority of pixels corresponding to stand replacing disturbance, while at the same time minimizing errors of omission and commission. For example, pixels representing leave patches in the T2 image will likely have rank difference values close to zero, whereas pixels representing newly constructed roads or landings in the T2 image will likely have large positive difference values. In the analysis described here, a threshold minimum is therefore used to avoid inclusion of vegetation that has not changed (lower end of the rank difference distribution), while a threshold maximum is used to avoid identifying all roads and landings (at the upper end of the rank difference distribution) as stand replacing disturbance. If our objective was to identify both stand replacing disturbances and all new road construction within our study area, a maximum threshold would likely not be necessary.

To facilitate threshold selection, 10% of these pixel values were selected at random. The mean and standard deviation the rank-order difference values were then iteratively used to determine the threshold for each image source. It was found that by using the mean value of the rank difference distribution ± 1 standard deviations, the stand replacing disturbances could be identified in all of the image sources (Table 3 and Figure 6). All pixel values having rank difference values within the threshold range, for each T2 image, were extracted, placed in a separate data layer, and labeled as stand replacing disturbance events. The application of the threshold resulted in many small areas or single pixel units identified as change. Many of these areas corresponded to locations where new roads had been constructed or where there was a potential spatial misregistration between the T1 and T2 images. These small change units were filtered out with the same operational criteria used in the construction of the VRI data (a 2 ha minimum mapping unit) (Resources Inventory Committee, 2002). As a result, all of the disturbance events that remained were greater than 2 ha in size.

4.1 Validation

A polygon decomposition process (Wulder and Franklin, 2001) was used to organize the stand replacing disturbance events identified by the rank-order change process to the corresponding forest inventory polygon (VRI). Table 4 summarizes the validation results. The first two columns of Table 4 characterize the VRI data and indicate the unique id and area (ha) of the VRI polygon. The next 3 columns characterize the manually delineated disturbance information by the year of the disturbance, area (ha), and proportion of the corresponding VRI polygon that was harvested. The subsequent columns summarize the area (ha) and proportion of the corresponding VRI polygon that were labeled as stand replacing disturbance through the rank-order change detection process. For example, VRI polygon #17272, with an area of 37 ha, was, according to the manual delineation, 100% harvested in 2000. The rank differencing approach using the ASTER image (2000), indicates that 78% of the polygon was harvested. This difference in area reported by the manual delineation and the change detection approach may be attributed to the fact that the manually delineated disturbance would generalize conditions on the ground by lumping all features, such as leave patches and roads, into the disturbance polygon, while the image-based change detection approach captures more spatially discrete units of change - and with the threshold range applied, excludes extreme difference values that are not directly associated with the removal of vegetation cover. For polygon #17272, the proportion of the polygon identified as having been disturbed diminishes over time, likely due to either reforestation or re-establishment of natural vegetation over time; the SPOT-4 (2003) and Landsat-5 (2004) images identified 64% and 55% respectively of the VRI polygon as disturbed.

VRI polygon #45917 was also 100% harvested in 2004. Related harvesting activity may have occurred in 2003 however, as the SPOT-4 (2003) data identified that 6% of polygon #45917 was disturbed that year. It is worth noting that in an operational forestry context, harvest blocks do not always align with stand boundaries as defined as the forest inventory. There are several reasons for this: first, the VRI is a strategic inventory delivered at a scale of 1:20,000, which provides an inadequate level of detail and spatial precision for operational harvesting plans. Secondly, there may be issues in how the original VRI polygon was delineated (e.g. the interpreter incorporated a swamp into the stand polygon, and it is unlikely that this area of the stand would be harvested); and finally, there may be operational or management constraints associated with harvesting certain areas of the stand. All of these factors, combined with the aforementioned difference in spatial representation inherent in raster and vector data sources, result in the variability in the proportion of the polygon that is disturbed.

Overall, Table 4 indicates that the rank-order change process applied to the corresponding year of the remotely sensed imagery successfully identified all of the stand replacing disturbances occurring in any given year. Figure 7 illustrates the proportion of each VRI polygon that was identified as change by each of the image sources. For example, all of the stand replacing disturbance events that occurred in 2000 were identified in the ASTER (2000) imagery. In addition, some disturbances occurring after August 2000 were also detected with ASTER (2000) for some VRI polygons that were subsequently harvested in 2003 or 2004, indicating capture of pre-harvesting access (road building) developments. Figure 7 illustrates the challenge associated with characterizing dynamic change on the landscape, where even for stand replacing disturbance, the change may manifest over several years. Four commission errors occurred where stand replacing disturbances were identified by the rank-order change detection process, but where the manual delineation did not identify any change events. These errors are noted in the last 4 rows of Table 4 (polygons #8344, #8454, #8781, #45951).

4.3 Land cover updating

Figure 8 illustrates the process followed to update an existing land cover product based on the outputs generated from the rank-order normalization and change detection procedure. Figure 8(A) and (B) depict the pre- and post-forest harvest scenes acquired from Landsat-7 and SPOT-4 platforms, respectively. Figure 8(C) details a subset of the EOSD land cover legend, as it pertains to the area under investigation, while Figure 8(D) shows the EOSD land cover product, representing land cover conditions in this area circa 2000. The change output generated from the rank-order process is shown in Figure 8(E) and finally, the updated EOSD land cover is shown in Figure 8(F). In this example, the type of disturbance and spectral clues from the T2 image aid in label assignment.

5.0 DISCUSSION

Regardless of the change detection approach followed, some form of image normalization is invariably required to ensure that detected changes result from physical changes in the target, rather than differences in image properties. For example, Paolini et al. (2006) found that change detection methods applied to non-corrected image pairs resulted in estimates of change in broad land cover classes that were two to three times greater than estimates obtained with corrected imagery. Similarly, Nelson et al. (2005) found changes in forest cover were difficult to detect when using non-normalized imagery. The need to normalize images must be weighed against the effort and cost required to complete the normalization (Cohen et al., 1998), and some consideration must also be given to the objective of the change detection (e.g., to identify stand replacing disturbance or identify all changes in forest cover) when assessing the need for normalization (Cohen et al., 2002).

The information received at a sensor includes measurements of reflected solar energy, and is inherently influenced by such factors as the spectral band response function, solar zenith angle, and sun-object-sensor orientation. More importantly, when analyzing multi-temporal imagery from the same sensor, environmental variables such as atmospheric conditions, topography, surface moisture, and seasonal phenology all influence the signal received at the sensor (Coops et al., 2006). When analyzing multi-temporal imagery from different sensors, all of the aforementioned factors must be considered as well as additional factors such as differences in the spectral and spatial resolutions of sensors, and in cross-sensor calibration coefficients must also be considered.

Normalizing multiple dates of imagery from the same sensor can be accomplished through either absolute or relative radiometric normalization techniques (Song and Woodcock, 2003). Absolute normalization (or image calibration) attempts to calibrate multiple images to a standard radiometric scale that results in comparable units such as surface reflectance (Peddle et al., 2003) and is often performed as a two-step process involving calibration coefficients that are used to convert at-sensor radiance to planetary reflectance, followed by the use of a radiative transfer model to derive surface reflectance based on *in situ* atmospheric measurements. In cases where no atmospheric data or sensor calibration data is available (especially when using historic image data), relative radiometric normalization is applied to match two or more scenes to one another based on an arbitrary scale such as scaled radiance or digital number (Yuan and Elvidge, 1996; Hall et al., 1991). This approach has been used to radiometrically normalize imagery to create seamless, large-area mosaics (Du et al., 2001), to estimate multi-temporal and multi-sensor defoliation in the boreal forest (Heikkila et al., 2002), to test change detection in forested environments (Chen et al., 2005; Nelson et al., 2005) and to derive a seamless mosaic of northern Canada from Landsat imagery (Olthof et al., 2005).

Normalizing multiple dates of imagery from multiple sensors is complicated by the differences in spatial and spectral resolution, and in sensor calibration coefficients. These complexities may explain why there are so few cross-sensor studies that have appeared in the literature. Landsat is fairly robust, and much effort has been focused on studying the relative calibration of each instrument (Teillet, et al., 2001; Teillet et. al. 2006). Examples of multi-sensor change detection are becoming more common due to the limited availability of data from older sensors or data from sensors that have stopped collecting data due to technical or administrative concerns (Serra et al., 2003). Cross-sensor normalization attempts to remove differences between multi-sensor images that are due to non-surface factors (Heo and FitzHugh, 2000). With the launch of Landsat-7 ETM+ in 1999, much of the multi-sensor research has focused on cross-calibration between the ETM+ sensor and earlier Landsat sensors (TM or MSS) to provide a consistent radiometric record from the extensive archive of Landsat imagery collected since 1972 (Teillet et al., 2004; Roder et al., 2005). Several studies have made use of the robust cross-calibration between Landsat sensors to characterize long-term trends in rangeland coverage (Hostert et al., 2003), post-fire vegetation dynamics (Chen et al., 2005), and patterns of forest succession (Schroeder et al., 2006; Song et al., 2007).

Data continuity is an important consideration for long-term monitoring programs and the unavailability of desired imagery from a particular sensor can restrict the goals of such a program. A multi-sensor change detection procedure, such as the rank-order change process demonstrated in this study, could be used to develop and analyze a suite of potential satellite sensors for long-term change detection studies. The approach shown here is ideal for detecting change in studies involving multi-temporal datasets where problems may arise due to relative image normalization or cross-sensor absolute radiometric calibration and issues around data continuity.

In this study, we applied a method of change detection, which addressed the issue of normalization of imagery collected with different sensors, and facilitated generation of change outputs. We applied an ordinal rank normalization procedure after Nelson et al. (2005) to multi-temporal imagery acquired from four different satellite sensors (Landsat-5 TM, Landsat-7 ETM+, ASTER, and SPOT-4) and use image differencing to detect changes between image dates. The normalization procedure employed in this method does not require extensive information on atmospheric parameters or the subjective selection of pseudo-invariant features. Each pixel is assigned a rank, relative to all other pixels in the image. The rank values for the image pairs are then subtracted and a threshold is applied to the difference values.

There are however several caveats associated with the use of the rank-order normalization change detection procedure. Firstly, as with many change detection studies, analysis of the results at the individual pixel level should be avoided, as the change maps are inherently noisy due to misregistration between image dates or differences in spatial resolution. Although this issue restricts the size of the change events that the procedure will resolve, as illustrated in this study, the trade-off is a more accurate change map at a slightly coarser spatial resolution. Furthermore, the use of existing data sets and operational mapping criteria provide a realistic context for the change detection. In this study, the existing forest inventory data and requirements for minimum mapping unit sizes were used pragmatically to capture the change events of interest.

Secondly, change thresholding is a somewhat subjective operation that should be strengthened through the use of pre- and post-disturbance ground surveys. Although this type of data was not available in this study, future work using this normalization procedure for change detection can be made more operational given calibration measurements on the ground to measure disturbance characteristics. The ability to use the statistical distribution of the data to determine a threshold, and to be able to apply the same standard criteria for the threshold (i.e., the mean ± 1 standard deviation) is advantageous in a multi-date, multi-sensor study such as this. For instance, 8-bit images only allow for a range of 256 possible values and the resultant normalized image may reveal many tied ranks, which may be an issue when using imagery with a narrow dynamic range or when attempting to discern subtle changes. Such issues merit further investigation over larger spatial extents. A related opportunity for additional research is in the investigation of rank-order change detection to detect a broader range of disturbance types. Further, the map update approach can be made increasingly sophisticated through use of context information (i.e., disturbance type) and spectral information (T2 class).

6.0 CONCLUSIONS

The main objective of this study is to capture stand-replacing disturbances across a forested landscape using data from multiple remote sensing platforms. Normalizing multiple dates of imagery from multiple sensors is complicated not only by factors relating to atmospheric conditions and sun-object-sensor illumination geometry but also by differences in spatial and spectral resolution, and at-sensor calibration coefficients. In this study, we attempt to minimize multi-temporal, multi-sensor differences by applying a rank-order change detection approach to derive change maps from Landsat-5, ASTER and SPOT-4 sensors, using an earlier baseline Landsat-7 image as reference. The rank-order change detection process may be most useful for applications involving multi-temporal and multi-sensor datasets where there is insufficient information for image normalization and cross-sensor radiometric calibration, or where data from the desired sensor is unavailable. The results of in this study show that methods for cross-sensor change may be developed that meet a particular application need, such as mapping stand replacing disturbance.

Limitations to cross-sensor change detection include: the absence of a spatially or temporally extensive image archive for the majority of sensors other than Landsat; small and/or incompatible image footprints and the associated processing overhead; and data distribution, policy, and cost. These logistical issues are likely to have a greater impact on further developments in cross-sensor change detection than issues of a purely scientific nature, and further emphasize the on-going need, particularly in the context of land cover applications, to promote and ensure continuity of the Landsat program and sensors.

Acknowledgements

We would like to thank David Seemann and Sarah McDonald of the Canadian Forest Service for assistance with initial data processing. Ann Morrison, of the BC Ministry of Forests and Range, is thanked for making available the forest inventory data used for calibration and validation of our change maps. Funding support of the Government Related Initiatives Program (GRIP) of the Canadian Space Agency is also acknowledged.

References

Allen, T.R. and Kupfer, J.A. 2001. Spectral response and spatial pattern of Fraser fir mortality and regeneration, Great Smoky Mountains, USA. *Plant Ecology*, *156*, 59-74.

British Columbia Ministry of Forests and Range. 2007. *Change detection for spatial VRI currency checking*. Available online (accessed February 1, 2007): http://www.for.gov.bc.ca/hts/rs/detection/index.html

Burt, J.E. and Barber, G.M. 1996. *Elementary Statistics for Geographers*. (New York: The Guilford Press).

Chen, X., Vierling, L. and Deering, D., 2005. A simple and effective radiometric correction method to improve landscape change detection across-sensors and across time. *Remote Sensing of Environment, 98*, 63-79.

Cohen, W.B., Fiorella, M., Gray, J., Helmer, E., and Anderson, K. 1998. An efficient and accurate method for mapping forest clearcuts in the Pacific Northwest using Landsat imagery. *Photogrammetric Engineering and Remote Sensing, 64,* 293-300.

Cohen, W.B., Spies, T.A., Alig, R.J., Oetter, D.R., Maiersperger, T.K., Fiorella, M. 2002. Characterizing 23 years (1972-95) of stand replacement disturbance in Western Oregon Forests with Landsat imagery. *Ecosystems, 5*, 122-137.

Cohen W. and Goward, S., 2004. Landsat's role in ecological applications of remote sensing. *BioScience*, *54*, 535-545.

Coops, N.C., Wulder, M.A., White, J.C. 2006. Identifying and describing forest disturbance and spatial pattern: data selection issues and methodological implications. Pages 31-62 in Wulder, M.A. and Franklin, S.E. (Editors). *Understanding Forest Disturbance and Spatial Pattern*. CRC Press: Boca Raton, FL. 246 p.

Coppin, P., Jonckheere, I., Nackaerts, K., Muys, B. and Lambin, E., 2004. Digital change detection methods in ecosystem monitoring: a review. *International Journal of Remote Sensing*, *25*, 1565-1596.

Desclée, B., Bogaert, P. and Defourny, P., 2006. Forest change detection by statistical object-based method. *Remote Sensing of Environment*, *102*, 1-11.

Du, Y, Cihlar, J., Beaubien, J and Latifovic, R. 2001. Radiometric Normalization, Compositing, and Quality Control for Satellite High Resolution Image Mosaics over Large Areas. *IEEE Transactions on Geoscience and Remote Sensing*, *39*, 623-634.

Epting, J., Verbyla, D., Sorbel, B. 2005. Evaluation of remotely sensed indices for assessing burn severity in interior Alaska using Landsat TM and ETM+. *Remote Sensing of Environment*, *96*, 328-339.

Falkenstrom, H. and Ekstrand, S. 2002. Evaluation of IRS-1C LISS-3 satellite data for defoliation assessment on Norway spruce and Scots pine. *Remote Sensing of Environment*, *82*, 208-223.

Fedpausch, T.R., McDonald, A.J., Passos, C.A.M., Lehman, J., Riha, S.J. 2006. Biomass, harvestable area, and forest structure estimated from commercial timber inventories and remotely sensed imagery in southern Amazonia. *Forest Ecology and Management*, *233*, 121-132.

Feranec, J., Hazeu, G., Christensen, S., and Jaffrain, G. 2007. Corine land cover change detection in Europe (case studies of the Netherlands and Slovakia). *Land Use Policy*, *24*, 234-247.

Food and Agriculture Organization of the United Nations. 2005. *Global Forest Resources Assessment 2005*. Available online (accessed February 1, 2007): http://www.fao.org/forestry/foris/webview/forestry2/index.jsp?siteId=101&sitetreeId=1191&langId=1&geoId=0

Foody, G.M. 2003. Remote sensing of tropical forest environments: Towards the monitoring of environmental resources for sustainable development. *International Journal of Remote Sensing*, *24*, 4035–4046

Franklin, S.E. and Wulder, M.A. 2002. Remote sensing methods in medium spatial resolution satellite data land cover classification of large areas. *Progress in Physical Geography*, *26*, 173-205.

Frederick, M. 2005. Latest Landsat 5 problem elevates data gap worries. *Space News*, December 6 2005.

Geomatics Canada, 1996. *Standards and specifications of the National Topographic Database Edition 3.18*. Sherbrooke, Que. Canada: Minister of Supply and Services Canada (CATALOGUE NO M52-70/1996).

Gong, P., B. Xu, 2003. Remote sensing of forests over time: change types, methods, and opportunities. Pages 301-333 in Wulder, M.A. and Franklin, S.E. (Editors). *Remote Sensing of Forest Environments: Concepts and Case Studies*, Kluwer Press, Amsterdam, Netherlands. 519 p.

Goward, S.N. and Skole, D.L. 2005. Landsat 2005: Time To Act. *Space News*, October 31 2005.

Hall, F., Strebel, D.E., Nickeson, Goetz, S.J. 1991. Radiometric rectification: Toward a Common Radiometric Response Among Multi-date, Multi-sensor Images. *Remote Sensing of Environment*, *35*, 11-27.

Hansen, A.J., Neilson, R.P., Dale, V.H., Flather, C.H., Iverson, L.R., Currie, D.J. Shafer, S., Cook, R., and Bartlein, P.J. 2001. Global change in forests: responses of species, communities, and biomes. *Bioscience*, *51*, 765-779.

Hayes, D.J. and Cohen, W.B. 2007. Spatial, spectral and temporal patterns of tropical forest cover change as observed by with multiple scales of optical data. *Remote Sensing of Environment*, *106*, 1-16.

Healey, .S.P, Yang, Z., Cohen, W.B. and Pierce, D.J. 2006a. Application of two regression-based methods to estimate the effects of partial harvest on forest structure using Landsat data. *Remote Sensing of Environment*, *101*, 115-126.

Healey, S.P., Cohen, W.B. Yang, Z. and Kennedy, R. 2006b. Remotely Sensed Data in the Mapping of Forest Harvest Patterns, in Wulder, M.A. and Franklin, S.E. (Editors). *Understanding Forest Disturbance and Spatial Pattern*. CRC Press: Boca Raton, FL. 246 p.

Heo, J. and FitzHugh, T.W. 2000. A Standardized Radiometric Normalization Method for Change Detection Using Remotely Sensed Imagery. *Photogrammetric Engineering and Remote Sensing, 66*, 173-181.

Heikkila, J., Nevalainen, S. and Tokola, T., 2002. Estimating defoliation in boreal coniferous forests by combining Landsat TM, aerial photographs and field data. *Forest Ecology and Management, 158,* 9-23.

Heiskanen, J. 2006. Estimating aboveground tree biomass and leaf area index in a mountain birch forest using ASTER satellite data. *International Journal of Remote Sensing, 27,* 1135-1158.

Hickey, G.M., Innes, J.L., Kozak, R.A., Bull, G.Q., Vertinsky, I. 2005. Monitoring and information reporting for sustainable forest management: an international multiple case study analysis. *Forest Ecology and Management, 209*, 237-259.

Hostert, P., Roder, A., and Hill, J. 2003. Coupling spectral unmixing and trend analysis for monitoring of long-term vegetation dynamics in Mediterranean rangelands. *Remote Sensing of Environment, 87,* 183-197.

Irish, R.R. 2000. Landsat 7 Science Data User's Handbook. Report 430-15-01-003-0. National Aeronautics and Space Administration, http://ltpwww.gsfc.nasa.gov/IAS/handbook/handbook_toc.html

Jensen, J.R. 2000. Remote Sensing of Environment, Prentice Hall, Upper Saddle River, NJ (2000).

Jin, S. and Sader, S.A. 2005. Comparison of time-series tasselled cap wetness and the normalized difference moisture index in detecting forest disturbances. *Remote Sensing of Environment, 94*, 364-372.

Langevin, C., and Snow, D.A. 2004. Identifying change in a dynamic urban landscape: a neural network approach to map-updating. *Progress in Planning, 61,* 327-348.

Lu, D., Mausel, P., Bronzdizio, E., and Moran, E. 2004. Change detection techniques. *International Journal of Remote Sensing, 25*, 2365-2407.

Mack, P.E. 1990. Viewing the Earth: The Social Construction of the Landsat Satellite System. Massachusetts Institute of Technology: Cambridge, MA.

Malingreau, J.P. 1993. Satellite monitoring of the world's forests: A review. Unasylva, 44:

Markham, B.L., Storey, J.C., Williams, D.L., and Irons, J.R. 2004. Landsat Sensor Performance: History and Current Status. *IEEE Transactions on Geoscience and Remote Sensing, 42*, 2691-2694.

Mas, J. F. (1999). Monitoring land-cover changes: A comparison of change detection techniques. *International Journal of Remote Sensing, 20,* 139–152.

McMichael, C.E., Hope, A.S., Roberts, D.A., and Anaya, M.R., 2004. Post-fire recovery of leaf area index in California chaparral: a remote sensing-chronosequence appraoch. *International Journal of Remote Sensing, 25,* 4743-4760.

Medinger, D., Pojar, J., (Editors). 1991. Ecosystems of British Columbia. Research Branch. British Columbia Ministry of Forests, Special Report Series No. 6, Victoria British Columbia.

Michener, W.K. and Houhoulis, P.F. 1997. Detection of vegetation changes associated with extensive flooding in a forested ecosystem. *Photogrammetric Engineering and Remote Sensing*, *63*, 1363-1374.

Muchoney, D.M and Haack, B.N., 1994. Change detection for monitoring forest defoliation. *Photogrammetric Engineering and Remote Sensing*, *60*, 1243-1251.

Muukkonen, P. and Heiskanen, J. 2005. Estimating biomass for boreal forests using ASTER satellite data combined with standwise forest inventory data. *Remote Sensing of Environment*, *99*, 434-447.

Natural Resources Canada. 2006. The State of Canada's Forests 2005-2006. Canadian Forest Service, Natural Reources Canada, Ottawa, Ontario, Canada. http://www.nrcan.gc.ca/cfs/national/what-quoi/sof/sof06/pdf/State-of-Forests_E.pdf

Nelson, T., Wilson, H.G., Boots, B. and Wulder, M.A., 2005. Use of ordinal conversion for radiometric normalization and change detection. *International Journal of Remote Sensing*, *26*, 535-541.

Nemmour, H. and Chibani, Y. 2006. Fuzzy neural network architecture for change detection in remotely sensed imagery. *International Journal of Remote Sensing, 27*, 705-717.

Olthof, I., Butson, C, Fernandes, R., Fraser, R., Latifovic, R. and Orazietti, J. 2005. Landsat ETM+ mosaic of northern Canada. *Canadian Journal of Remote Sensing*, *31*, 412-419.

Paolini, L., Grings, F., Sobrino, J.A., Jimenez Munoz, J.C. and Karszenbaum, H. 2006. Radiometric correction effects in Landsat multi-date/multi-sensor change detection studies. *International Journal of Remote Sensing, 27,* 685-704.

Peddle, D.R., P.M. Teillet and M.A. Wulder, 2003. Radiometric Image Processing. Pages 181-208 in Wulder, M.A. and Franklin, S.E., (Editors) *Remote Sensing of Forest Environments: Concepts and Case Studies*, Kluwer Press, Amsterdam, Netherlands. 519 p.

Prenzel, B.G. and Treitz, P. 2006. Spectral and spatial filtering for enhanced thematic change analysis of remotely sensed data. *International Journal of Remote Sensing, 27,* 835-854.

Price, K.P. and Jakubauskas, M.E. 1998. Spectral retrogression and insect damage in lodgepole pine successional forests. *International Journal of Remote Sensing, 19,* 1627-1632.

Resources Inventory Committee. 2002. *Vegetation Resources Inventory, Photo Interpretation Procedures, Version 2.4, March 29, 2002*. Ministry of Sustainable Resource Management, Terrestrial Information Branch. Resources Inventory Committee,Victoria BC.

Roder, A., Kuemmerle, T., and Hill, J., 2005. Extension of retrospective datasets using multiple sensors. An approach to radiometric intercalibration of Landsat TM and MSS data. *Remote Sensing of Environment, 95*, 195-210.

Rogan, J., Franklin, J. and Roberts, D., 2002. A comparison of methods for monitoring multitemporal vegetation change using Thematic Mapper imagery. *Remote Sensing of Environment, 80*, 143-156.

Schroeder, T.A., Cohen, W.B., Song, C., Canty, M.J. and Yang, Z. 2006. Radiometric correction of multi-temporal Landsat data for characterization of early successional forest patterns in western Oregon. *Remote Sensing of Environment 103,* 16-26.

Serra, P., Pons, X. and Sauri, D., 2003. Post-classification change detection with data from different sensors: some accuracy considerations. *International Journal of Remote Sensing*, *24*, 3311-3340.

Singh, A. 1989. Digital change detection techniques using remotely sensed data. *International Journal of Remote Sensing*, *10*, 989-1003.

Skakun, R. S., Wulder, A. M, Franklin S. E., 2003. Sensitivity of the thematic mapper enhanced wetness difference index to detect mountain pine beetle red-attack damage. *Remote Sensing Environment*, *86*, 433-443.

Song, C. and Woodcock, C.E. 2003. Monitoring forest succession with multitemporal Landsat images: factors of uncertainty. *IEEE Transactions on Geoscience and Remote Sensing*, *41*, 2557-2567.

Song, C., Schroeder, T., Cohen, W.B. 2007. Predicting temperate conifer forest successional stage distributions with multitemporal Landsat Thematic Mapper imagery. *Remote Sensing of Environment*, *106*, 228-237.

SPOT Image, 2006. Online archive: http://www.spotimage.fr/html/_167_194_710_.php

Teillet, P.M., Markham, B.L., Irish, R.R. 2006. Landsat cross-calibration based on near simultaneous imaging of common ground targets. *Remote Sensing of Environment*, *102*, 264-270.

Teillet, P.M., Helder, D.L., Ruggles., T.A., Landry, R., Ahern, F.J., Higgs, N.J., Barsi, J., Chander, G., Markham, B.L., Barker, J.L., Thome, K.J., Schott, J.R. and Palluconi, F.D. 2004. A definitive calibration record for the Landsat-5 thematic mapper anchored to the Landsat-7 radiometric scale. *Canadian Journal of Remote Sensing*, *30*, 631-643.

Teillet, P.M., Barker, J.L., Markham, B.L., Irish, R.R., Fedosejevs, G., and Storey, J.C. Radiometric cross-calibration of the Landsat-7 ETM+ and Landsat-5 TM sensors based on tandem data sets. 2001. *Remote Sensing of Environment*, *78*, 39-54.

Treitz, P. and Rogan, J., 2004. Remote sensing for mapping and monitoring land-cover and land-use change: An introduction. *Progress in Planning*, *61*, 269-279.

United States Geological Service. 2007. National Landsat Archive Production System (NLAPS). EROS Data Center, http://edc.usgs.gov/guides/images/landsat_tm/nlaps.html

Wilson, E.H. and Sader, S.A. 2002. Detection of forest harvest type using multiple dates of Landsat TM imagery. *Remote Sensing of Environment*, *80*, 385-396.

Woodcock, C.E., Macomber, S.A., Pax-Lenney, M., Cohen, W.B. 2001. Monitoring large areas for forest change using Landsat: Generalization across space, time, and Landsat sensors. *Remote Sensing of Environment*, *78*, 194-203.

Wulder, M., Franklin, S.E. 2001. Polygon decomposition with remotely sensed data: Rationale, methods, and applications, *Geomatica*, *55*, 11-21.

Wulder, M.A., Dechka, J.A., Gillis, M.A., Luther, J.E., Hall, R.J., Beaudoin, A. and Franklin, S.E. 2003. Operational mapping of the land cover of the forested area of Canada with Landsat data: EOSD land cover program. *Forestry Chronicle*, *79*, 1075-1083.

Wulder, M.A., Kurz, W.A., Gillis, M. 2004. National level forest monitoring and modeling in Canada. *Progress in Planning*, *61*, 365-381.

Wulder, M.A., Dymond, C.C., White, J.C., Leckie, D.G. and Carroll, A.L., 2006. Surveying mountain pine beetle damage of forests: A review of remote sensing opportunities. *Forest Ecology and Management*, *221*, 27-41.

Yuan, D., and Elvidge, C.D., 1996. Comparison of relative radiometric normalization techniques. *Journal of Photogrammetric Engineering and Remote Sensing*, *51*, 117-126.

Table 1. Study image data.

Sensor	Acquisition Date	Spatial Resolution (m)	NIR Spectral Resolution (μm)
Landsat-7 ETM+	September 12, 1999	30	0.75 - 0.90
ASTER	August 4, 2000	15	0.78 - 0.86
SPOT-4	August 8, 2003	20	0.79 - 0.89
Landsat-5 TM	July 15, 2004	30	0.75 - 0.90

Table 2. A summary of the manually interpreted stand replacing disturbance events and the corresponding VRI polygons.

Date Range and Data Sources	Count of stand replacing disturbance polygons	Area (ha)	Number of VRI polygons	VRI polygon area (ha)
1999-2000 Landsat 7 ETM+ (1999) and ASTER (2000)	5	144	6	202
1999-2003 Landsat 7 ETM+ (1999) and SPOT-4 (2003)	23	739	23	754
1999-2004 Landsat 7 ETM+ (1999) and Landsat-5 TM (2004)	3	102	4	115

Table 3. A summary of information used for threshold determination.

Image	Year	Total # of Pixels	Sample Size	Mean	Standard Deviation	Lower Threshold	Upper Threshold
ASTER	2000	1599	160	114860	64554	50306	179414
SPOT-4	2003	8172	817	125695	60855	64840	186550
Landsat-5	2004	1133	113	122612	54215	68397	176827

Table 4. A complete listing of the polygon decomposition results of the manually interpreted stand replacing disturbance, and output from the rank-order change detection process for the ASTER, SPOT-4, and Landsat-5 TM data.

VRI			DISTURBANCE DATA		ASTER (2000)		SPOT-4 (2003)		LANDSAT-5 (2004)	
VRI#	AREA (ha)	YEAR	AREA (ha)	% of VRI POLY	AREA (ha)	% of VRI POLY	AREA (ha)	% of VRI POLY	AREA (ha)	% of VRI POLY
17272	37	2000	37	100	29	78	24	64	21	55
45898	53	2000	29	56	20	38	23	43	21	41
45940	45	2000	28	63	15	33	16	35	15	32
45945	37	2000	19	53	9	24	12	32	12	34
45947	22	2000	22	100	8	36	10	46	9	39
45948	8	2000	8	100	5	66	3	43	4	45
45896	35	2003	35	100	3	7	20	57	17	50
45897	9	2003	9	100	0	3	6	64	5	52
45899	15	2003	15	100	0	2	12	79	10	67
45900	18	2003	18	100	1	3	14	82	14	81
45901	15	2003	9	61	0	2	7	49	7	44
45909	27	2003	27	100	0	0	17	64	15	55
45912	23	2003	23	100	0	0	17	75	12	53
45913	30	2003	30	100	0	0	18	60	13	43
45916	15	2003	15	100	0	0	10	66	8	57
45924	40	2003	40	100	0	0	33	82	29	73
45925	41	2003	41	100	0	1	29	70	15	36
45927	17	2003	17	100	1	7	12	69	7	39
45931	7	2003	7	100	0	2	6	79	5	65
45932	33	2003	33	100	1	4	24	73	12	38
45933	7	2003	7	100	0	0	2	32	1	12
45937	17	2003	17	100	0	2	5	27	4	26
45938	35	2003	35	100	2	6	30	85	29	82
45939	117	2003	98	83	6	5	69	58	64	54
45944	96	2003	96	100	5	5	65	67	19	20
45946	27	2003	27	100	0	0	12	45	11	41
45949	52	2003	52	100	1	1	24	45	18	35
45950	51	2003	51	100	5	10	39	76	24	47
45952	27	2003	27	100	1	2	24	88	24	89
45915	43	2004	30	71	1	1	2	6	19	45
45917	45	2004	45	100	1	2	3	6	23	51
45921	13	2004	6	44	0	1	0	3	4	32
45935	15	2004	9	62	0	2	1	7	7	46
8344	8	0	0	0	3	37	1	13	1	11
8454	8	0	0	0	2	30	0	1	0	1
8781	8	0	0	0	3	36	0	4	1	7
45951	6	0	0	0	1	17	2	38	1	22

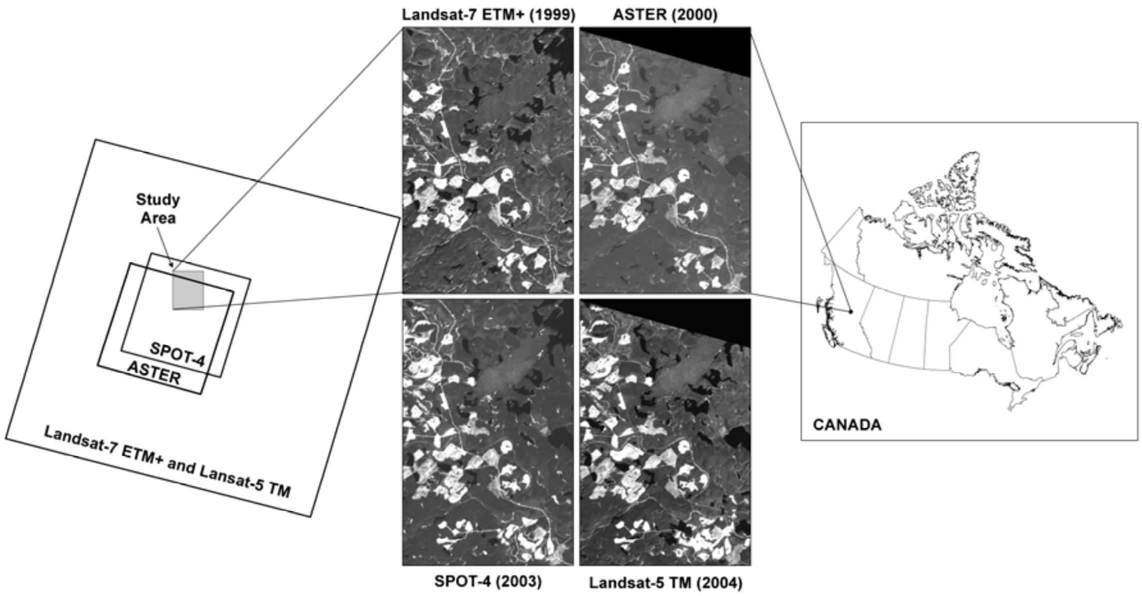

Figure 1. Image extents for the Landsat-7 ETM+, ASTER, SPOT-4, and Landsat-5 TM (420 by 650 pixels). The NIR band for each image is shown (see Table 1 for spectral range of NIR). The ASTER and SPOT-4 images were resampled to a 30 meter spatial resolution to match the Landsat images.

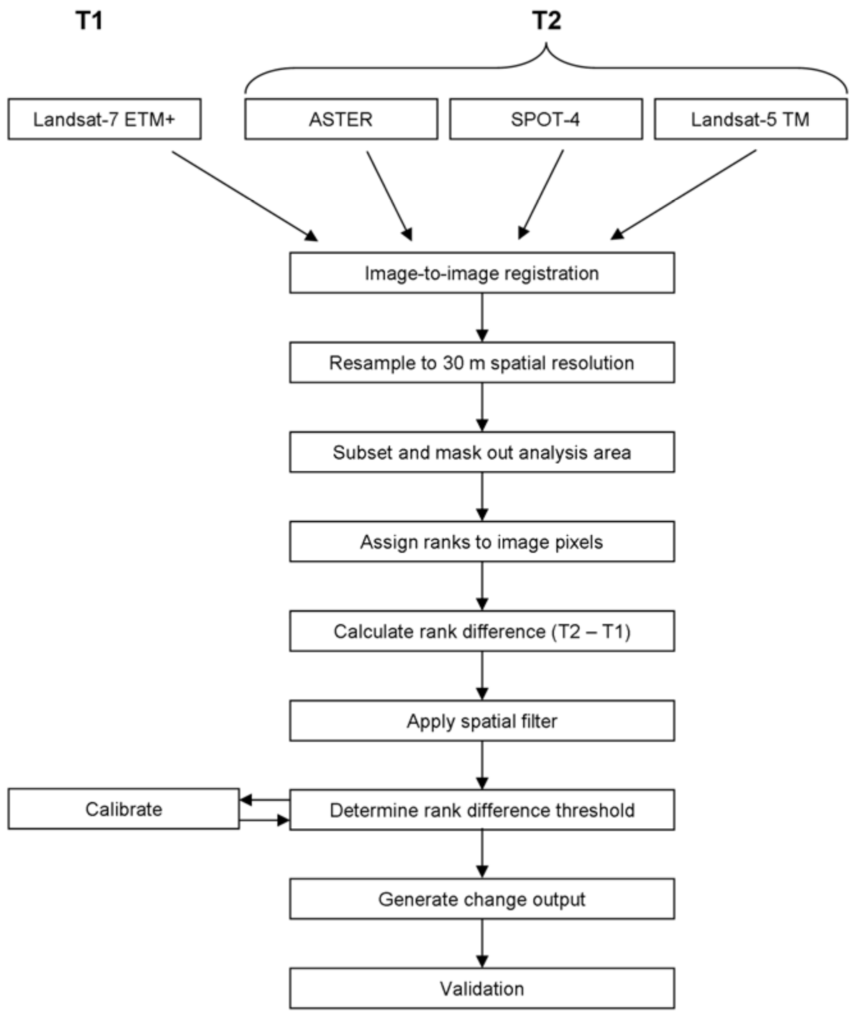

Figure 2. Flowchart illustrating the change detection steps.

A. Extract pixel values.

Pixel Location x	y	Pixel Value
1	1	8
1	2	5
1	3	4
1	4	5
1	5	1
...	...	...
n	n	#

B. Sort pixel values in ascending order.

Pixel Location x	y	Pixel Value
1	5	1
1	3	4
1	2	5
1	4	5
1	1	8
...	...	...
n	n	#

C. Assign ordinal ranks.

Pixel Location x	y	Pixel Value	Pixel Rank
1	5	1	1
1	3	4	2
1	2	5	3.5
1	4	5	3.5
1	1	8	5
...	...	...	...
n	n	#	#

Figure 3. The rank-order normalization procedure.

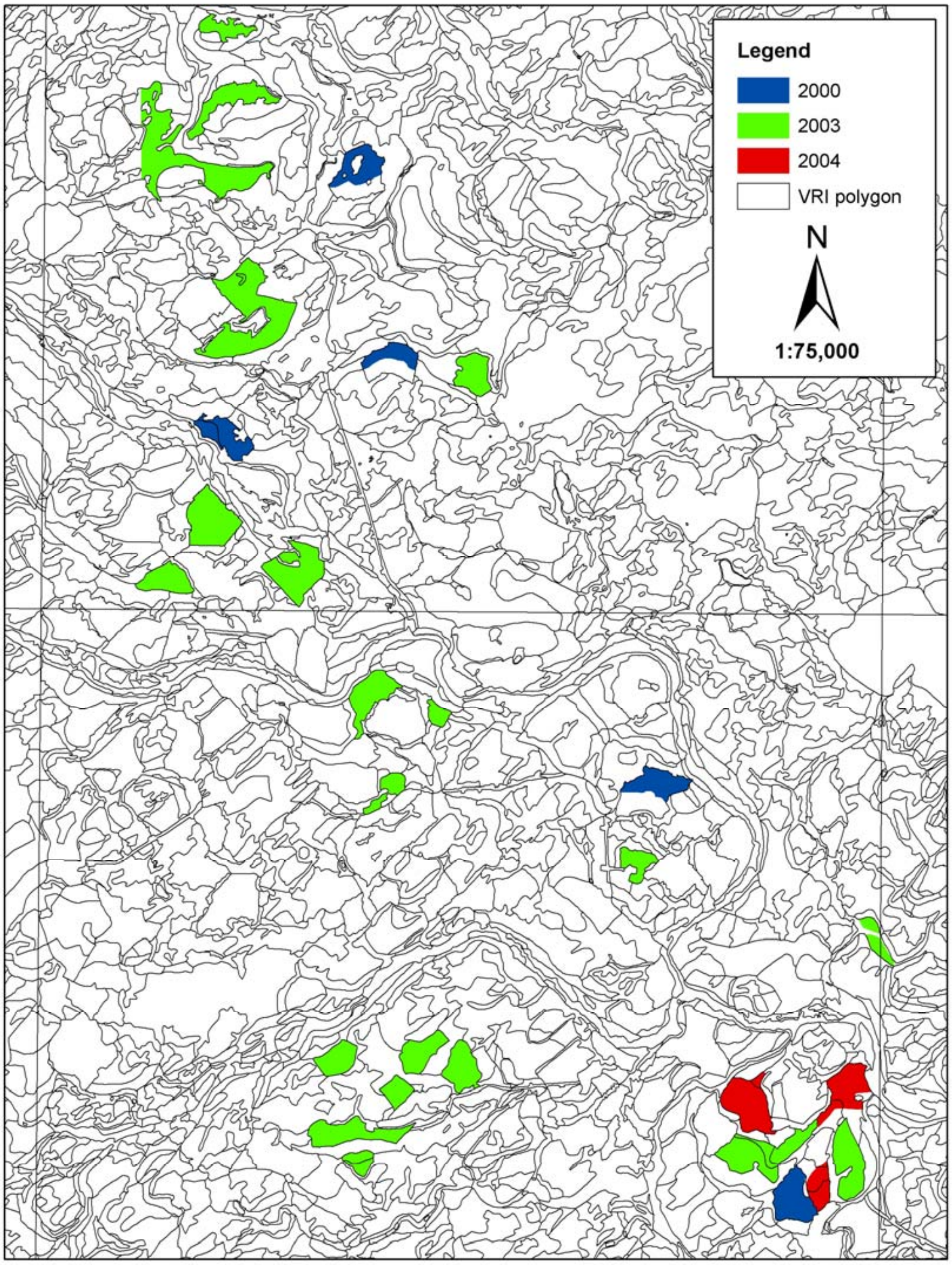

Figure 4. Forest inventory data with location and year of stand replacing disturbance.

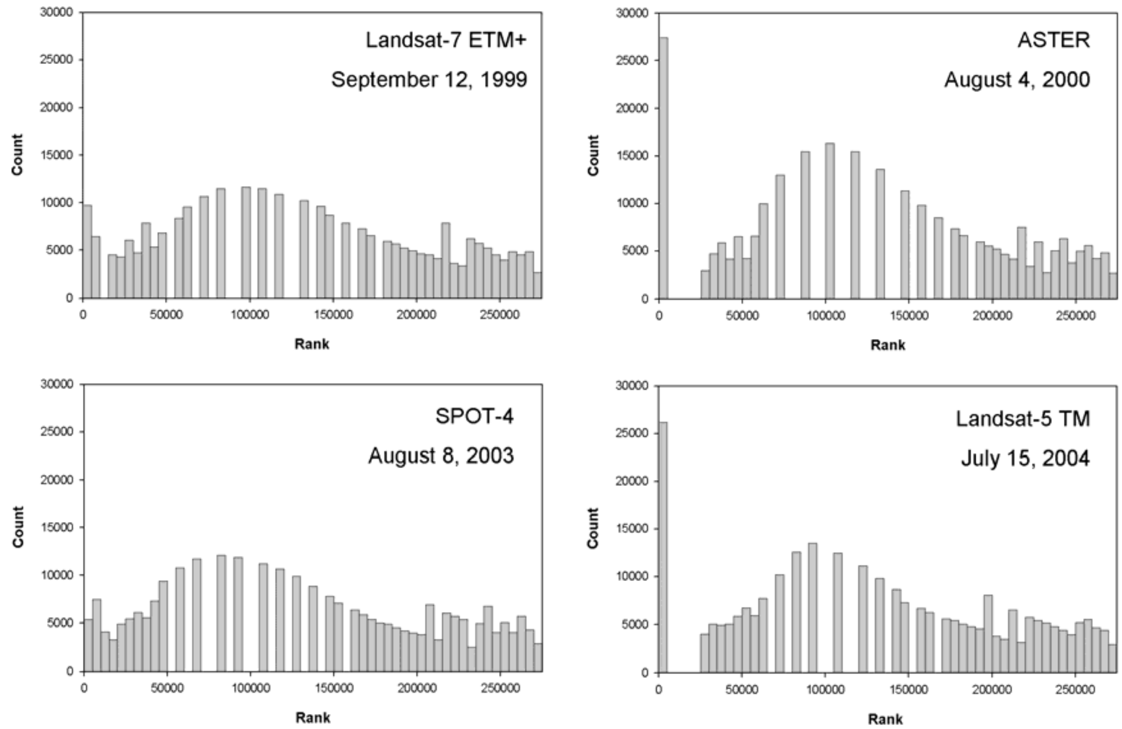

Figure 5. Distribution of rank pixel values for the NIR band from each of the image sources.

Landsat-7 ETM+ (1999) - ASTER (2000):
Distribution of Rank Difference Values for Stand Replacing Disturbances in 2000

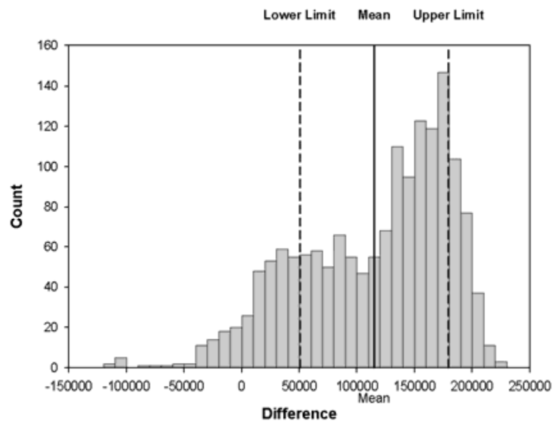

Landsat 7 ETM+ (1999) - SPOT-4 (2004):
Distribution of Rank Values for Stand Replacing Disturbances in 2003

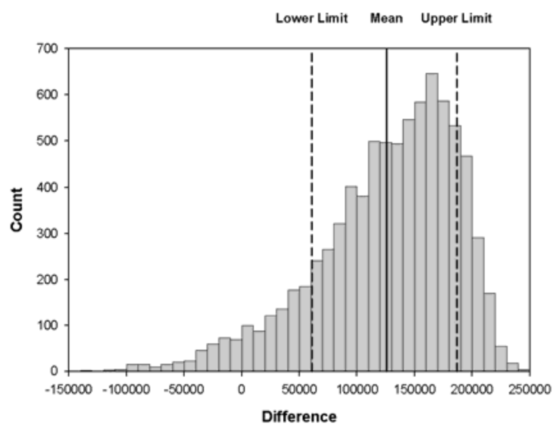

Landsat 7 ETM+ (1999) - Landsat-5 TM (2004):
Distribution of Rank Values for Stand Replacing Disturbances in 2004

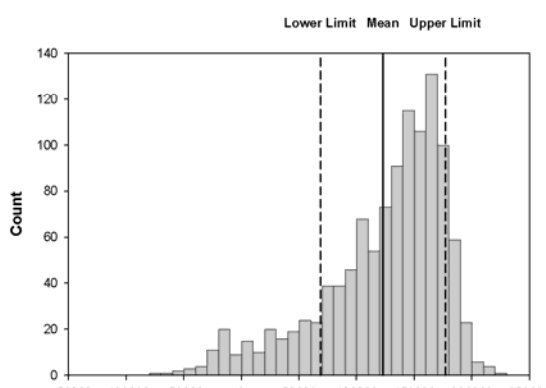

Figure 6. Distribution of the rank-order difference values within stand replacing disturbances for each of the T1 and T2 image pairs with threshold ranges indicated.

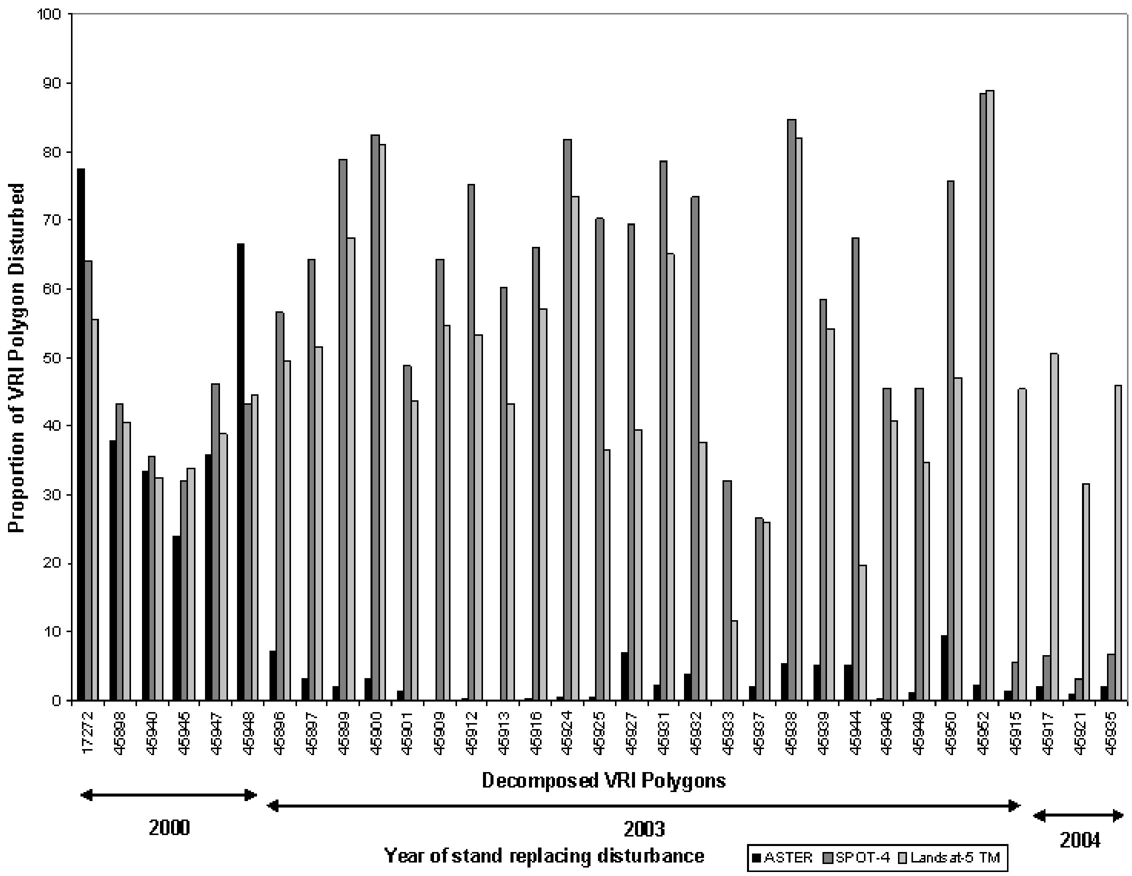

Figure 7. Proportion of forest inventory polygons identified as disturbed by the ASTER, SPOT-4, and Landsat-5 TM imagery.

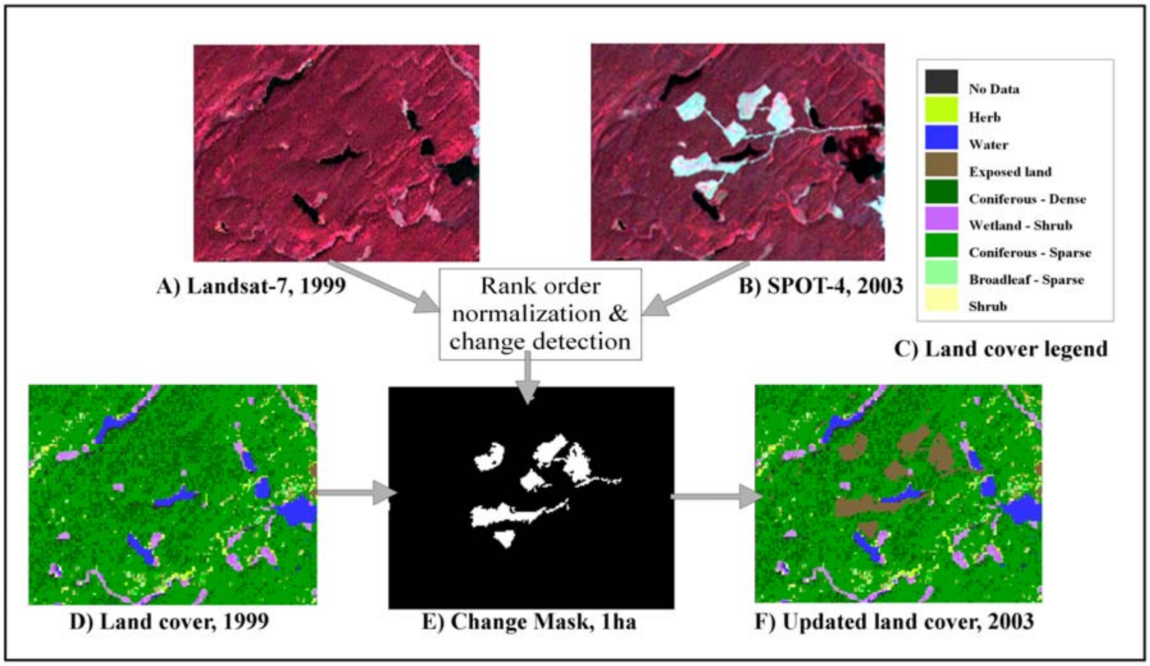

Figure 8. Updating a land cover map based on change areas derived from SPOT-4 imagery from 2003. A. Landsat-7 image, 1999. B. SPOT-4 image, 2003. C. EOSD land cover legend. D. Land cover circa 2000. E. Change Mask filtered to 1ha. F. Updated land cover map, circa 2003.